Supplemental Online Content

Taddei RN, Perbet R, Mate de Gerando A, et al. Tau Oligomer-Containing Synapse Elimination by Microglia and Astrocytes in Alzheimer Disease. Published online October 9, 2023. *JAMA Neurol*. doi:10.1001/jamaneurol.2023.3530

This supplemental material has been provided by the authors to give readers additional information about their work.

eMethods.

Commented [TS1]: The eReferences and citations have been reordered and renumbered starting from 1 (per our style) based on the order in which they were cited in the eMethods. Please double-check for accuracy.

Commented [TRN2R1]: Thank you. That is great.

1. Quantitative Assessments of Aβ-Plaques, Neuropil Threads, and γH2AX Burden

Brain tissue sections containing visual cortex derived from formalin-fixed paraffin-embedded tissue blocks were cut at a thickness of 7 µm. Immunohistochemical staining with DAB was conducted using a Bond RX autostainer from Leica Biosystems. We used primary antibodies to label Aβ deposits (4G8, Bio Legend, 1:8000), phospho-tau positive neuropil threads (AT8, Thermo Fisher, 1:500), and cellular DNA damage (γH2AX, Abcam, 1:1000). Slides were scanned with a Nanozoomer XR (NDP.scan 3.3.3, Hamamatsu Photonics, Hertfordhsire, UK) using a 20X objective. To quantify lesions, we used an artificial intelligence (AI) based semi-automated quantification method (Aiforia version 5.2, Aiforia Inc, Cambridge, MA) following our previously described protocol [1]. Aβ-plaque burden (defined as the percentage of cortex occupied by Aβ-plaques), density of neuropil threads/mm^2, and density of γH2AX + cells/mm^2 were calculated (Supplement Figure 1). To quantify tau neuropil burden, slides stained with AT8 antibody were analyzed using the QuPath software [2] with the use of the pixel classifier module.

2. Steps of Expansion Microscopy (ExM) Protocol

Preparation of glass-slide mounted FFPE sections: 25 µm-thick formalin-fixed paraffin embedded human brain sections from the visual cortex (Brodmann areas 17/18) were deparaffinized in xylene (2 x 5mins) and rehydrated in decreasing ethanol concentrations 100%-95%-90%-80%-50%-ddH2O (2 x 5mins each). Slides were dried at room temperature. A 0.5 mm thick silicon isolator (Grace Bio Labs, catalog number NC1652199) was placed on top of the slide to fully surround the tissue section. Anchoring step: AcX solution was prepared diluting the AcX stock to 1:100 in Triton-PBS (0.5%). 500 µl of freshly prepared AcX solution was placed on top of the slide covering the tissue until reaching the borders of the silicon isolator. The anchoring solution was left incubating overnight in a humidified environment at room temperature. The next day the slide was washed in PBS (3 x 5mins) and left to dry at room temperature. Gelling step: Gelling solution was freshly prepared on the same day. For 500 µl gelling solution 467.5 µl of monomer solution (2.5% acrylamide, 8.6% sodium acrylate, and 0.1% N-N-methylenebisacrylamide, diluted in distilled water), 10 µl of 4HT, 10 µl of TEMED, and 12.5 µl of APS were added in this sequential order to an Eppendorf tube. The gelling solution was immediately placed on top of the slide and a gel chamber was created by placing a glass coverslip (24x40mm, Thermo Fisher, catalog number 102440) on top of the silicon isolator. The gelling solution was incubated overnight in a humidified environment at room temperature. Digestion step: The glass coverslip and silicon isolator were carefully removed. The gel was trimmed with a razor blade up to the edges of the tissue. Gel not covering the tissue was removed. The trimmed gels, still mounted on the glass slide, were placed in 50ml Falcon tubes. Digestion buffer was prepared adding beta-mecaptoethanol (0.7%) to the digestion stock (5% 1M Tris, 5% 500mM EDTA, 0.5% Triton-X, 20% SDS, diluted in distilled water). A heat-detergent digestion was performed in an autoclave at 121°C for 60 mins. The samples were left to cool down inside the autoclave for at least 6 hours. Gel processing: Gels now detached from the glass slides were carefully removed from the Falcon tubes and washed in PBS (3 x 5mins). Gels were measured to obtain the `expansion factor 1' shown in eFigure 2 in Supplement and incubated in Trueblack Plus (Biotium, catalog number 23014) diluted in PBS (1:140) for 48 hours in a humidified environment at room temperature to quench autofluorescence and to better visualize gray and white matter boundaries in the transparent gels. Gels were cut into ~0.5x0.5 cm small sections labelled as `cortex' and/or `WM' and placed into a 24-well plate (Greiner BioOne, Fisher Scientific, catalog number 07000680). Immunostaining: Primary and secondary antibody stainings were performed inside the wells. Briefly, gel sections were blocked (MaxBlock, Active Motif) overnight at room temperature and washed in washing buffer (MaxWash, Active Motif) 3 x 10 mins. Primary antibodies were diluted at 1:100 in staining solution (MaxStain, Active Motif) and incubated for 24 to 48 hours at room temperature. Gel sections were washed in washing buffer (MaxWash, Active Motif) 3 x 10mins, prior to incubation with secondary antibodies (Alexa 405, Alexa 488, Alexa 555, Alexa 647) diluted at 1:100 in staining solution (MaxStain, Active Motif) overnight at room temperature. Gel sections were washed in washing buffer (MaxWash, Active Motif) 3 x 10mins and incubated in ddH2O for 24hs to allow for maximal expansion of the tissue. Gel pieces were measured to obtain the `expansion factor 2' shown in eFigure 2 in Supplement prior to imaging. For long-term storage, gels were placed in PBS and stored at 4°C. Expansion factor: Total expansion factor was calculated by multiplying the `expansion factor 1' obtained after the digestion step by the `expansion factor 2' obtained after 24h incubation of gel pieces in ddH2O. The ExM obtained across all brains (N=28) was of 4.6x, which is in line with previous publications [3-6] (eFigure 2 in Supplement).

3. Preparation of Synaptosome and Cytosol-Enriched Fractions

300 mg of frozen human brain from the secondary visual cortex (Brodmann area 18) was gently homogenized with 25 strokes in a 2 ml Potter-Elvehjem tissue grinder in chilled 750 µl of buffer A (25 mM HEPES pH 7.5,

120 mM NaCl, 5 mM KCl, 1 mM MgCl2, 2 mM CaCl2 in distilled water, supplemented with 1 mM DTT and 1:100 phosphatase-/protease-inhibitor). The homogenate was passed through 2 layers of nylon 80 µm filters using 25 mm filter holders to remove tissue debris and was then passed through a 5 µm supor membrane to filter out large organelles and nuclei. The obtained homogenate was centrifuged at 1,000 × g for 10 min at 4°C. The supernatant was transferred into pre-CYT tubes, and the pellet was chilled in ice in pre-SYN tubes. The pre-CYT tubes were centrifuged at 10,000 × g for 15 min at 4°C to remove remaining debris and the supernatant was transferred to CYT tubes to obtain the final CYT samples. The pre-SYN tubes were washed with 500 µl Buffer A and equally divided into two tubes (pre-SYN-DTT and pre-SYN-PBS) and centrifuged at 1,000 × g for 10 min at 4°C to remove remaining debris. The pre-SYN pellets were resuspended in either 100 µl Buffer B1 (PBS, 1.5% SDS, 2 mM DTT, 1:100 phosphatase-/protease-inhibitor) to obtain the final SYN-DTT samples (used for reducing/denaturing Western blots) (Figure 3c and d and eFigure 7a-c in Supplement), or in 100 µl Buffer B2 (PBS, 1.5% SDS, 2 mM DTT, 1:100 protease-inhibitor) to obtain the final SYN-PBS samples (used for native Western blots) (Figure 3a and b). A bicinchoninic acid (BCA) assay (Thermo Scientific Pierce) was performed to determine total protein concentration.

4. Western Blotting (WB)

Reducing and denaturing WBs: Twenty to fifty micrograms of total protein were loaded per well on 4–12% Bis-Tris SDS-PAGE gels (Invitrogen) and run in MOPS buffer (Invitrogen) at 160 V for 1 hour. Samples were diluted in PBS, and loading and reducing agents were added. The samples were heated at 95°C for 5 mins prior to loading. Proteins were transferred to nitrocellulose membranes (Invitrogen) with an iBlot2 transfer device using a protocol of 25 V for 7 min. Membranes were incubated in blocking solution (Intercept Blocking buffer) for 1 hour at room temperature. Primary antibodies were diluted in antibody diluent (Intercept Antibody diluent) and incubated overnight at 4°C on a rotating plate. Blots were washed in Tris buffered saline + 0.25% Tween (TBS-T) 3 x 10min and incubated with infrared and/or horseradish peroxidase (HRP) secondary antibodies at 1:5000 dilution in antibody diluent (Intercept Antibody diluent) for 1 h at room temperature. Blots were washed in TBS-T 3 x 10 min and imaged with an Odyssey CLx Infrared Imaging System for infrared secondary antibodies and/or a chemiluminescent BioRad ChemiDoc Imaging System for HRP secondary antibodies. Blots were converted to grayscale and densitometry analysis was performed with ImageJ (64-bit Java 8) (Figure 3c and d and eFigure 7a-c in Supplement).

Native WBs: Samples were prepared by dilution in PBS with addition of NativePage loading buffer and NativePAGE™ 5% G-250 Sample additive without reducing agent and/or sample heating. Sixty micrograms of total protein were loaded per well on NativePage 3–12% Bis-Tris gels (Invitrogen). Gels were run in NativePage anode and cathode running buffers at 150 V for 20mins followed by 170 V for 50mins after changing the cathode buffer. Proteins were transferred to PVDF membrane (Invitrogen) with an iBlot2 transfer device using a protocol of 20 V for 7 min. Membranes were quickly washed with methanol to remove the excess of blue and placed in acetic acid (8%) for 5 mins followed by ddH20 for 5 mins. Membranes were air-dried at room temperature. Blocking was performed with 5% non-fat dried milk diluted in TBS-T for 1 hour. Primary antibodies were diluted in 5% non-fat dried milk and incubated overnight at 4°C on a rotating plate. Blots were washed in TBS-T 3 x 10 min and incubated with HRP secondary antibody at 1:5000 dilution in 5% non-fat dried milk for 1h at room temperature. Blots were washed in TBS-T 3 x 10 min and imaged with high-sensitivity streptavidin-HRP (Thermo Fisher, catalog number 21134) on a chemiluminescent BioRad ChemiDoc Imaging System. Blots were converted to grayscale and densitometry analysis was performed in ImageJ (64-bit Java 8) (Figure 3a and b).

eReferences.

1. Taddei RN, Sanchez-Mico MV, Bonnar O, et al. Changes in glial cell phenotypes precede overt neurofibrillary tangle formation, correlate with markers of cortical cell damage, and predict cognitive status of individuals at Braak III-IV stages. *Acta Neuropathologica Communications*. 2022;10(1):72. doi:10.1186/s40478-022-01370-3

2. Bankhead P, Loughrey MB, Fernández JA, et al. QuPath: Open source software for digital pathology image analysis. *Scientific Reports*. 2017;7(1):16878. doi:10.1038/s41598-017-17204-5

3. Sherwood CC, Miller SB, Karl M, et al. Invariant Synapse Density and Neuronal Connectivity Scaling in Primate Neocortical Evolution. *Cerebral Cortex*. 2020;30(10):5604-5615. doi:10.1093/cercor/bhaa149

4. Domínguez-Álvaro M, Montero-Crespo M, Blazquez-Llorca L, Insausti R, DeFelipe J, Alonso-Nanclares L. Three-dimensional analysis of synapses in the transentorhinal cortex of Alzheimer's disease patients. *Acta Neuropathol Commun*. 2018;6(1):20-20. doi:10.1186/s40478-018-0520-6

5. Cragg BG. The density of synapses and neurons in normal, mentally defective and ageing human brains. *Brain*. 1975;98(1):81-90. doi:10.1093/brain/98.1.81

6. Shapson-Coe A, Januszewski M, Berger DR, et al. A connectomic study of a petascale fragment of human cerebral cortex. *bioRxiv*. Published online January 1, 2021:2021.05.29.446289. doi:10.1101/2021.05.29.446289

7. Vonsattel JPG, Myers RH, Tessa Hedley-Whyte E, Ropper AH, Bird ED, Richardson Jr EP. Cerebral amyloid angiopathy without and with cerebral hemorrhages: A comparative histological study. *Annals of Neurology*. 1991;30(5):637-649. doi:10.1002/ana.410300503

Table and Figure Legends

eTable 1. Antibodies Used in the Present Study
List of antibodies, host, clonality, distributor, catalogue number, and their respective dilutions used for expansion microscopy (ExM), Western Blot (WB), and immunohistochemistry/immunofluorescence (IHC/IF).

eTable 2. Baseline Demographic and Neuropathologic Characteristics of the Subset of N=10 Human Brains Studied
Demographic and neuropathologic features of the total N=10 subjects included in the analyses of TOC1+ pre- and postsynapses, and of microglial and astrocytic engulfment of TOC1-containing synapses (data is shown in Figure 4 and eFigure 8 in Supplement). Thal phase: No amyloid deposition (A0), amyloid in neocortex (A1), amyloid in allocortex/limbic region (A2), amyloid in diencephalon/basal ganglia (A3), amyloid in brainstem/midbrain (A4), amyloid in cerebellum (A5); CERAD score: No neuritic plaques (C0), sparse plaques (C1), moderate plaques (C2), frequent plaques (C3); Cerebrovascular composite score includes subscores for: hypertensive cerebrovascular, atherosclerosis, cerebral atherosclerosis, occlusive atherosclerosis and cerebral amyloid angiopathy score [7]; MMSE: Mini-Mental State Examination score; PMI: Postmortem interval; N: number; SD: Standard deviation. Respective p-values are shown in the graphs.

eFigure 1. **Neuropathologic Assessment of Amyloid-β and Tau Burdens in the Studied Brains**
Representative photomicrographs of Aβ-plaques, AT8+ neurofibrillary tangles and neuropil threads, and ɣH2AX stainings in the visual cortex of control, resilient, and demented cases (**a**), and semiquantitative analyses of 4G8+ Aβ plaque burden (**b**), AT8+ neuropil thread burden (**c**), and ɣH2AX+ cellular damage density (**d**) in the visual cortex of control, resilient, and demented brains. Burdens of Aβ plaques and of AT8+ neuropil threads in the visual cortex, defined as the percentage of cortex occupied by Aβ deposits immunostained with 4G8 antibody and AT8+ neuropil threads, respectively (**a**) did not significantly differ between demented and resilient brains (**b, c**). Density of ɣH2AX+ cells/mm^2 was significantly increased in demented compared to resilient and controls (**d**). C Control (Braak 0-II); R Resilient (Braak III/IV); D Demented (Braak III/IV); Scale bars 50 μm. Respective p-values are shown in the graphs.

eFigure 2. **Steps of Expansion Microsopy (ExM) Exemplified**
Example of the expansion microscopy (ExM) protocol method used in the present study. Slides and steps of the ExM protocol are exemplified with a brain section from the visual cortex (**a**); average expansion factor obtained after steps 1-3 (expansion factor 1: 2.2x), and after 24 h incubation in double-distilled (dd) H2O prior to imaging (expansion factor 2: 2.1x) to achieve a final total expansion factor 4.6x. (**b**). AcX: Acryloyl-X; BA: Brodmann Area.

eFigure 3. Synapse Densities Across Groups and Correlation Analyses Between Synapse Densities and Cognitive and Neuropathological Measures

Synapse densities were significantly reduced in the visual cortex of demented compared to resilient and control brains when assessing Synapsin1+ presynapses and PSD95+ postsynapses (**a**); loss of mature synapses was significantly correlated with antemortem WAIS-R subscore ('digit symbol substitution') (**b**) and with a marker of early cell damage (γH2AX) (**c**) in the visual cortex; Analyses shown were performed on N=28 brains. Synapse densities represented in the graphs correspond to the values obtained in expanded tissue sections and must be multiplied by a factor of ~100 (=4.6^3) to account for the 4.6x volume expansion factor achieved by the ExM protocol used here in order to extrapolate them to pre-expanded tissue material. C Control (Braak 0-II), N=6; R Resilient (Braak III/IV), N=8; D Demented (Braak III/IV), N=14; N: number. Respective p-values are shown in the graphs.

eFigure 4. Confocal Images of Engulfment of Synaptic Elements by Microglia and Astrocytes
Microglia and astrocytes engulfed significantly more Synapsin1+ presynapses, PSD95+ postsynapses and Synapsin1+/PSD95+ colocalized synapses in demented compared to resilient and control brains. Post-ExM with confocal imaging showing internalized synaptic elements inside IBA1+ ameboid microglial cells (**a2-a4**) and GFAP+ astrocytes (**a6-a8**). Example of an IBA1+ ameboid microglia and a GFAP+ astrocyte in blue (**a1, a5**) co-labelled with Synapsin1 in magenta (**a2, a6**) and PSD95 in green (**a3, a7**) showing each channel individually (**a1-a3, a5-a7**) and the merged image at the end (**a4, a8**). Scale bars 10 μm.

eFigure 5. **Expanded Astrocyte Co-Stained With a Cytoskeletal and a Cytoplasmic Antibody**
Representative images indicating colocalization of astrocytic intermediate-filament antibody GFAP (magenta) with cytoplasmic astrocytic antibody ALDH1L1 (green), showing that the GFAP antibody labels astrocyte-specific cell bodies and processes and that GFAP+ signal does not exceed the boundaries of ALDH1L1+ astrocytic staining. Arrows indicate GFAP+/ALDH1L1+ astrocytes and arrowheads GFAP-/ALDH1L1+ astrocytes. Scale bar 20 μm.

eFigure 6. **Lysosomal Co-Staining of Engulfed Synaptic Elements in Representative Microglia and Astrocyte**
IBA1+ microglia (**a1**) and GFAP+ astrocyte (**b1**) in blue co-labelled with PSD95+ postsynapses in green (**a1/a2, b1/b2**) and LAMP2+ lysosomes in red (**a1/3, b1/3**) showing glia-internalized PSD95+ elements colocalized with LAMP2+ lysosomes inside the microglial and astrocytic cell, respectively. Scale bars 5 μm (**a**) and 10 μm (**b**).

eFigure 7. Quality of Extracted Synaptosomes and Measures of Truncated Tau Species in Synaptosome Fractions
Synaptosome extractions and WB validation showing representative cytosolic (CYT) and synaptosome (SYN) fractions from three cases (1-3) using the presynaptic marker Synaptophysin (red) and the postsynaptic marker PSD95 (green) (**a**); WB analyses of synaptosome-enriched fractions from the visual cortex showed that tau truncation, as measured with N-terminal tau (Tau12) (**b**) and C-terminal tau (Tau46) (**c**), did not differ across demented, resilient, and control brains. Of note, WBs of synaptosome-enriched fractions with ptau217 showed no detectable signal and with AT180/ptau231 showed no difference across groups. Analyses were performed on N=21 synaptosome extractions (4 controls, 5

resilient, 12 demented), respectively. Arrowheads in black indicate the band width quantified for each of the WB analyses and respective antibodies; C/Ctrl Control (Braak 0-II); R/Res Resilient (Braak III/IV); D/Dem Demented (Braak III/IV); N:number; WB: Western Blot.

eFigure 8. Association of Oligomeric Tau With Synaptic Elements
TOC1+ tau oligomers were significantly increased in Bassoon+ presynapses and PSD95+ postsynapses of demented compared to resilient and control brains (**a, b**). Representative images showing colocalized Bassoon+/TOC1+ presynaptic puncta (white circles) in control, resilient and demented brains (**a**, first column) and colocalized PSD95+/TOC1+ postsynaptic puncta (white circles) in demented, resilient, and control brains (**a**, second column). Analyses were performed on N=10 brains (2 controls, 4 resilient, 4 demented); C Control (Braak 0-II); R Resilient (Braak III/IV); D Demented (Braak III/IV). Scale bar 5 μm. Respective p-values are shown in the graphs.

eTable 1. Antibodies Used in the Present Study

Antibody	Host, clonality	ExM	WB	IHC/IF	Distributor	Cat. Number
4G8	Mouse, monoclonal	1:100		1:8000	Bio Legend	800709
ALDH1L1	Mouse, monoclonal	1:100			EMD	MABN495
AT180	Mouse, monoclonal		1:200		Thermo Fisher	MN1040
AT270	Mouse, monoclonal		1:200		Thermo Fisher	MN1050
AT8	Mouse, monoclonal	1:100	1:1000	1:500	Thermo Fisher	MN1020
Bassoon	Mouse, monoclonal	1:100			Abcam	ab82958
GAPDH	Rabbit, monoclonal		1:1000		Cell Signaling	14C10
GFAP	Mouse, monoclonal	1:100			Sigma Aldrich	SAB4300647
GFAP	Rat, monoclonal	1:100			Abcam	ab279291
IBA1	Chicken, monoclonal	1:100			Synaptic Systems	140009
LAMP2	Rabbit, monoclonal	1:100			Abcam	ab199946
MAP2	Chicken, polyclonal	1:100			Abcam	ab5392
PSD95	Rabbit, monoclonal	1:100	1:1000		Cell Signaling	D74D3-3409S
PSD95	Mouse, monoclonal	1:100			Abcam	ab192757
Synaptophysin	Mouse, monoclonal		1:1000		Abcam	ab8049
Synapsin1	Rabbit, monoclonal	1:100			Abcam	ab254349
Tau p217	Rabbit, polyclonal		1:500		Thermo Fisher	44-744
Tau12 biotin	Mouse, monoclonal		1:500		BioLegend	806505
Tau46 biotin	Mouse, monoclonal		1:1000		Cell Signaling	96767
Tau5	Mouse, monoclonal		1:500		Abcam	ab80579
TOC1	Rabbit, monoclonal	1:100	1:500		Absolute Antibodies	Ab02650-23.0
Trueblack Plus	NA	1:140			Biotium	23014
yH2AX	Mouse, monoclonal			1:1000	Abcam	ab26350
Alexa Fluor 405	Donkey/Goat	1:100	1:5000		Invitrogen	A5760
Alexa Fluor 488	Donkey/Goat	1:100	1:5000		Invitrogen	A10436
Alexa Fluor 555	Donkey/Goat	1:100	1:5000		Invitrogen	A30677
Alexa Fluor 647	Donkey/Goat	1:100	1:5000		Invitrogen	A30107
HRP Streptavidin	NA		1:5000		Thermo Fisher	31030

List of antibodies, host, clonality, distributor, catalogue number, and their respective dilutions used for expansion microscopy (ExM), Western Blot (WB), and immunohistochemistry/immunofluorescence (IHC/IF).

eTable 2. Baseline Demographic and Neuropathologic Characteristics of the Subset of N=10 Human Brains Studied

Cognitive status	Control	Resilient	Demented	p
Number of subjects, total N=10	2	4	4	
Cognitive scores				
MMSE (mean, SD)	30 (0)	29.5 (0.6)	26 (1.6)	.04
Age (years)				
Mean (SD)	83 (9.9)	80.8 (3.6)	85.2 (8.8)	ns
Sex				
Female N (%)	1 (50%)	3 (75%)	3 (75%)	ns
Male N (%)	1 (50%)	1 (25%)	1 (25%)	ns
Neuropathology ('ABC' score)				
A-Thal phase, median (range)	0	2.5 (2-4)	4 (2-5)	ns
B-Braak stage, median (range)	1.5 (1-2)	3 (3-4)	3.5 (3-4)	ns
C-CERAD score, median (range)	0	1.5 (0-2)	1 (0-2)	ns
Vascular score				
Composite score, mean (SD)	5 (1.4)	2.8 (3)	2.7 (1.3)	ns
PMI (hours)				
Mean (SD)	24 (0)	25.5 (21.4)	22.7 (8.5)	ns

Demographic and neuropathologic features of the total N=10 subjects included in the analyses of TOC1+ pre- and postsynapses, and of microglial and astrocytic engulfment of TOC1-containing synapses (data is shown in Figure 4 and eFigure 8 in Supplement). Thal phase: No amyloid deposition (A0), amyloid in neocortex (A1), amyloid in allocortex/limbic region (A2), amyloid in diencephalon/basal ganglia (A3), amyloid in brainstem/midbrain (A4), amyloid in cerebellum (A5); CERAD score: No neuritic plaques (C0), sparse plaques (C1), moderate plaques (C2), frequent plaques (C3); Cerebrovascular composite score includes subscores for: hypertensive cerebrovascular, atherosclerosis, cerebral atherosclerosis, occlusive atherosclerosis and cerebral amyloid angiopathy score [7]; MMSE: Mini-Mental State Examination score; N: number; ns: not significant; PMI: Postmortem interval; SD: Standard deviation. Respective p-values are shown in the graphs.

eFigure 1. Neuropathologic Assessment of Amyloid-β and Tau Burdens in the Studied Brains

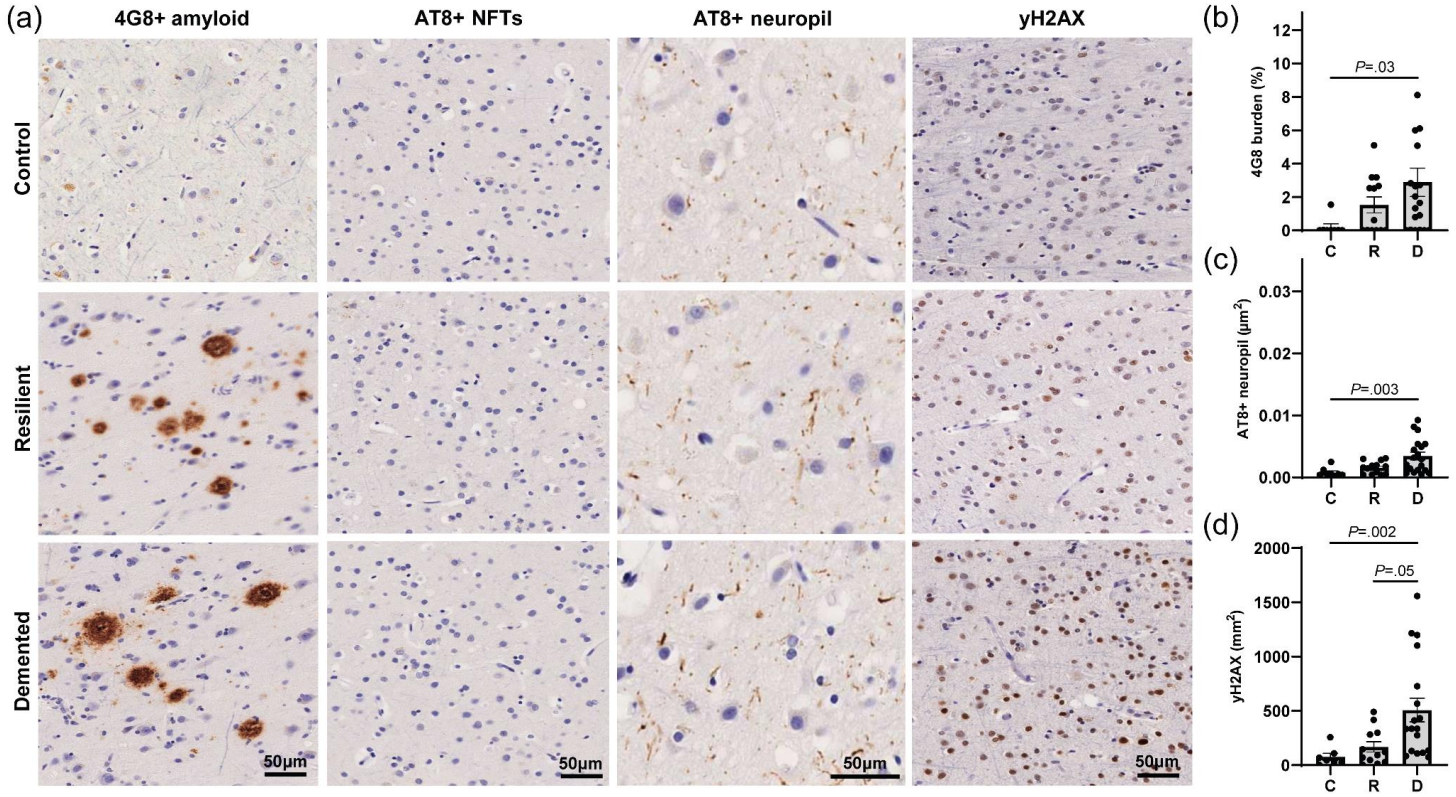

Representative photomicrographs of Aβ-plaques, AT8+ neurofibrillary tangles and neuropil threads, and γH2AX stainings in the visual cortex of control, resilient, and demented cases (**a**), and semiquantitative analyses of 4G8+ Aβ plaque burden (**b**), AT8+ neuropil thread burden (**c**), and γH2AX+ cellular damage density (**d**) in the visual cortex of control, resilient, and demented brains. Burdens of Aβ plaques and of AT8+ neuropil threads in the visual cortex, defined as the percentage of cortex occupied by Aβ deposits immunostained with 4G8 antibody and AT8+ neuropil threads, respectively (**a**) did not significantly differ between demented and resilient brains (**b, c**). Density of γH2AX+ cells/mm^2 was significantly increased in demented compared to resilient and controls (**d**). C Control (Braak 0-II); R Resilient (Braak III/IV); D Demented (Braak III/IV); Scale bars 50 µm. Respective p-values are shown in the graphs.

eFigure 2. Steps of Expansion Microscopy (ExM) Exemplified

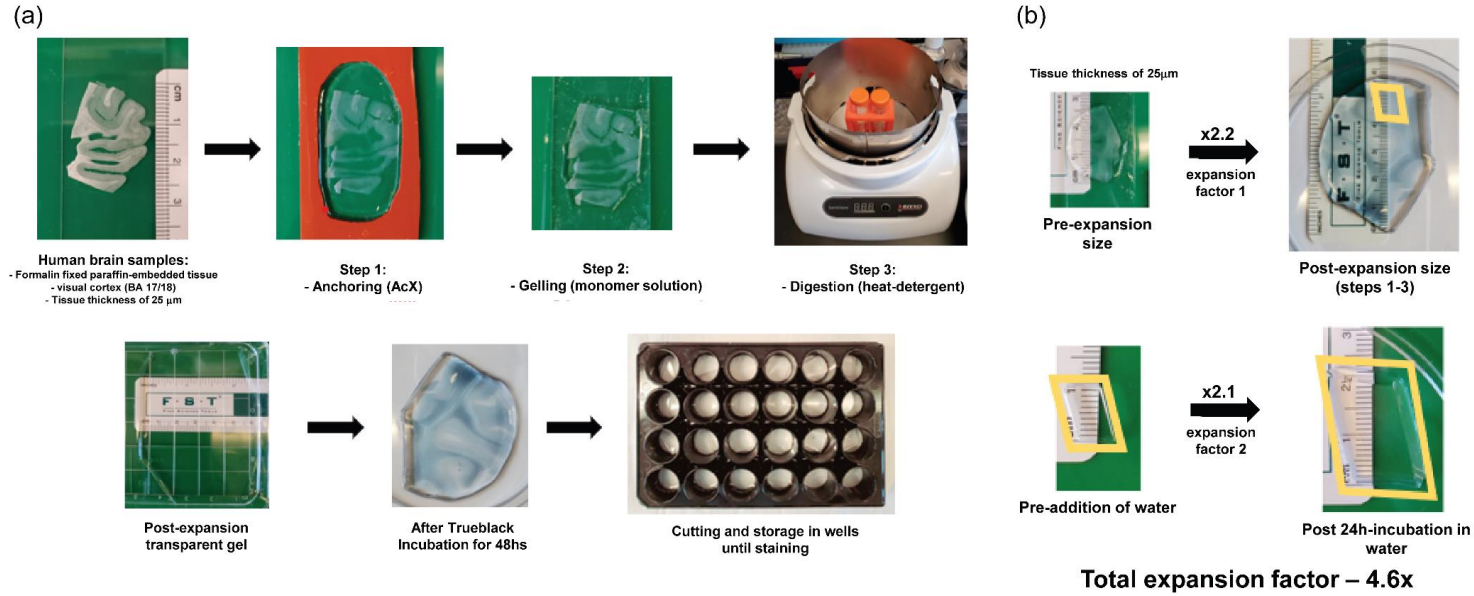

Example of the expansion microscopy (ExM) protocol method used in the present study. Slides and steps of the ExM protocol are exemplified with a brain section from the visual cortex (**a**); average expansion factor obtained after steps 1-3 (expansion factor 1: 2.2x), and after 24 h incubation in double-distilled (dd) H2O prior to imaging (expansion factor 2: 2.1x) to achieve a final total expansion factor 4.6x. (**b**). AcX: Acryloyl-X; BA: Brodmann Area.

eFigure 3. Synapse Densities Across Groups and Correlation Analyses Between Synapse Densities and Cognitive and Neuropathological Measures

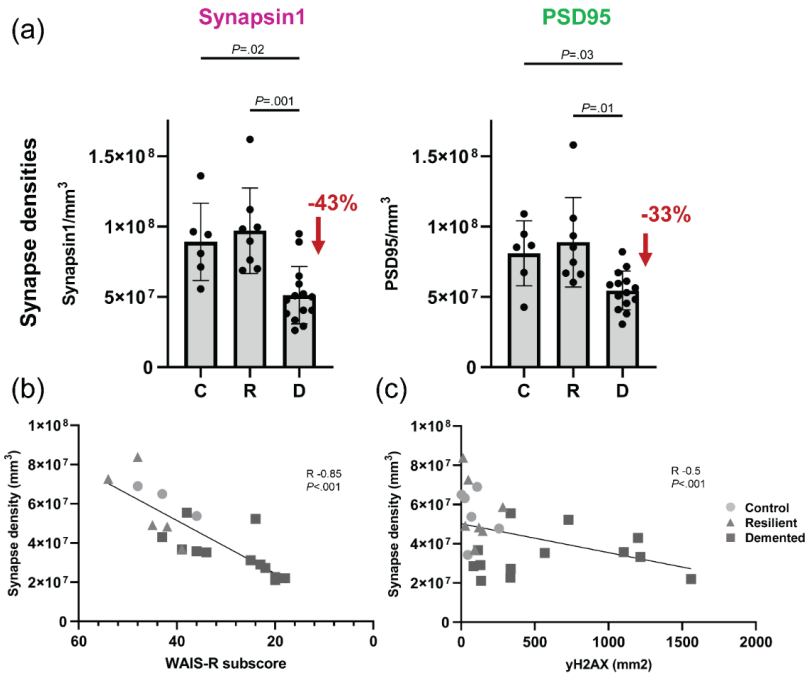

Synapse densities were significantly reduced in the visual cortex of demented compared to resilient and control brains when assessing Synapsin1+ presynapses and PSD95+ postsynapses (**a**); loss of mature synapses was significantly correlated with antemortem WAIS-R subscore ('digit symbol substitution') (**b**) and with a marker of early cell damage (γH2AX) (**c**) in the visual cortex; Analyses shown were performed on N=28 brains. Synapse densities represented in the graphs correspond to the values obtained in expanded tissue sections and must be multiplied by a factor of ~100 (=4.6^3) to account for the 4.6x volume expansion factor achieved by the ExM protocol used here in order to extrapolate them to pre-expanded tissue material. C Control (Braak 0-II), N=6; R Resilient (Braak III/IV), N=8; D Demented (Braak III/IV), N=14; N: number. Respective p-values are shown in the graphs.

eFigure 4. Confocal Images of Engulfment of Synaptic Elements by Microglia and Astrocytes

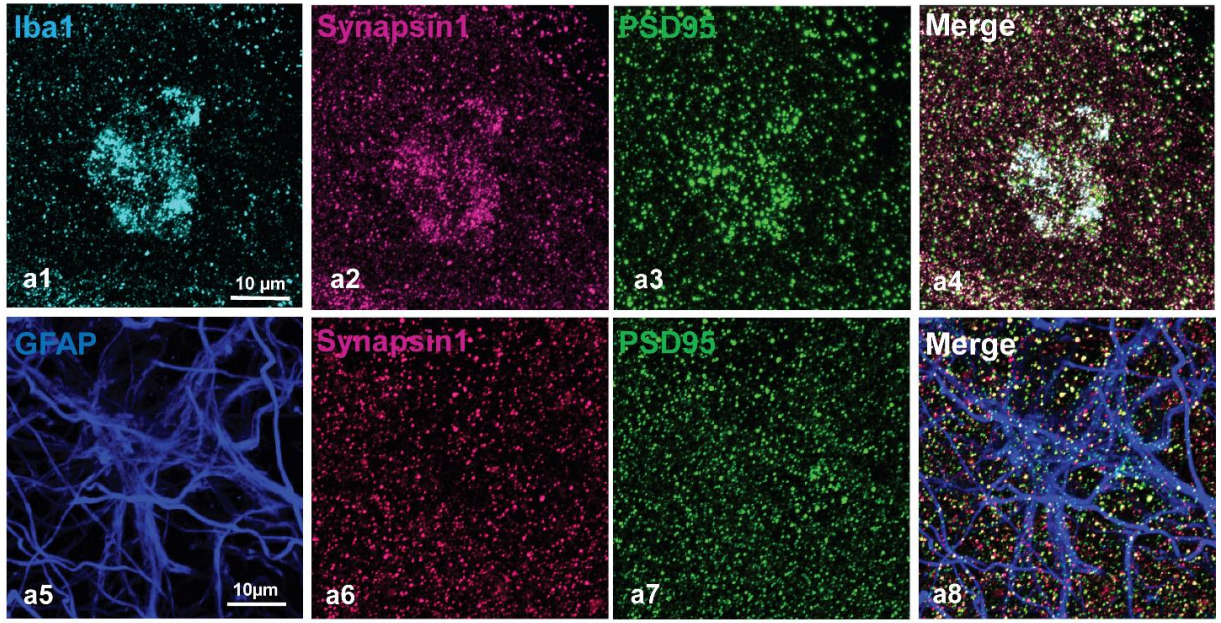

Microglia and astrocytes engulfed significantly more Synapsin1+ presynapses, PSD95+ postsynapses and Synapsin1+/PSD95+ colocalized synapses in demented compared to resilient and control brains. Post-ExM with confocal imaging showing internalized synaptic elements inside IBA1+ ameboid microglial cells (**a2-a4**) and GFAP+ astrocytes (**a6-a8**). Example of an IBA1+ ameboid microglia and a GFAP+ astrocyte in blue (**a1, a5**) co-labelled with Synapsin1 in magenta (**a2, a6**) and PSD95 in green (**a3, a7**) showing each channel individually (**a1-a3, a5-a7**) and the merged image at the end (**a4, a8**). Scale bars 10 µm.

eFigure 5. Expanded Astrocyte Co-Stained With a Cytoskeletal and a Cytoplasmic Antibody

Representative images indicating colocalization of astrocytic intermediate-filament antibody GFAP (magenta) with cytoplasmic astrocytic antibody ALDH1L1 (green), showing that the GFAP antibody labels astrocyte-specific cell bodies and processes and that GFAP+ signal does not exceed the boundaries of ALDH1L1+ astrocytic staining. Arrows indicate GFAP+/ALDH1L1+ astrocytes and arrowheads GFAP-/ALDH1L1+ astrocytes. Scale bar 20 µm.

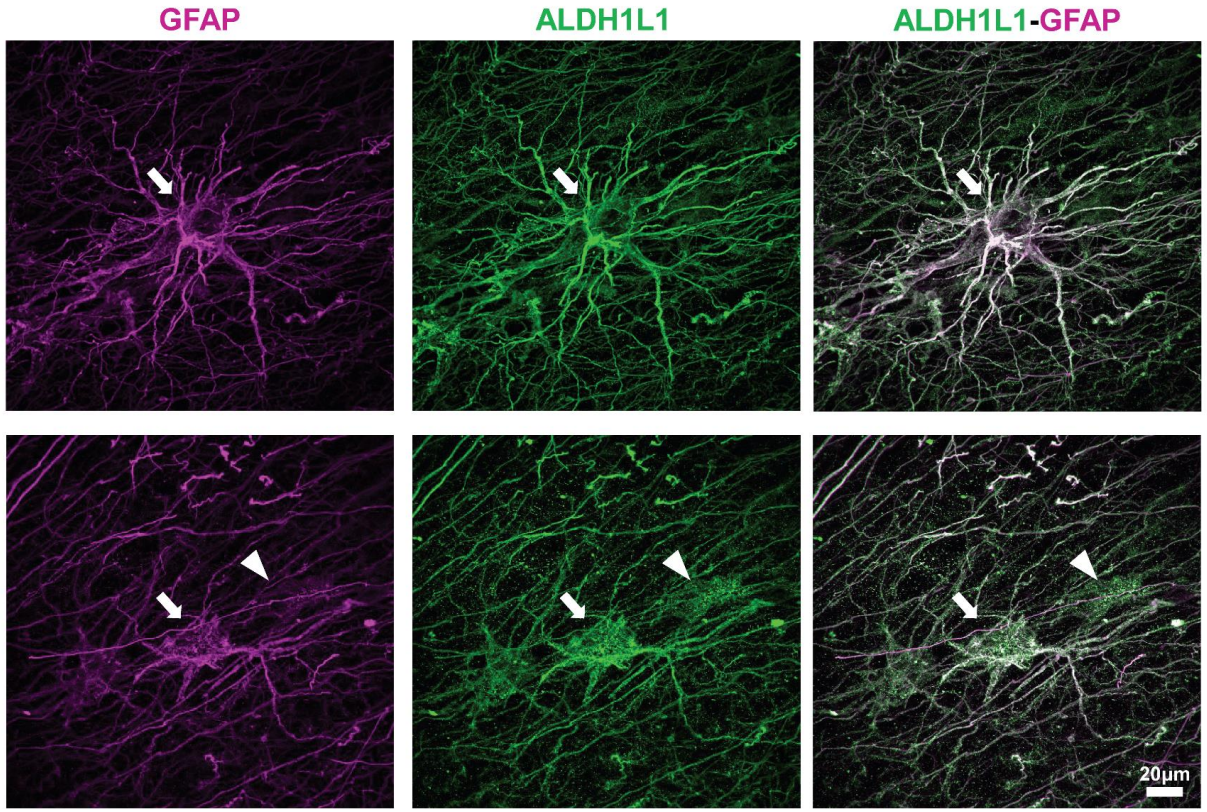

eFigure 6. Lysosomal Co-Staining of Engulfed Synaptic Elements in Representative Microglia and Astrocyte

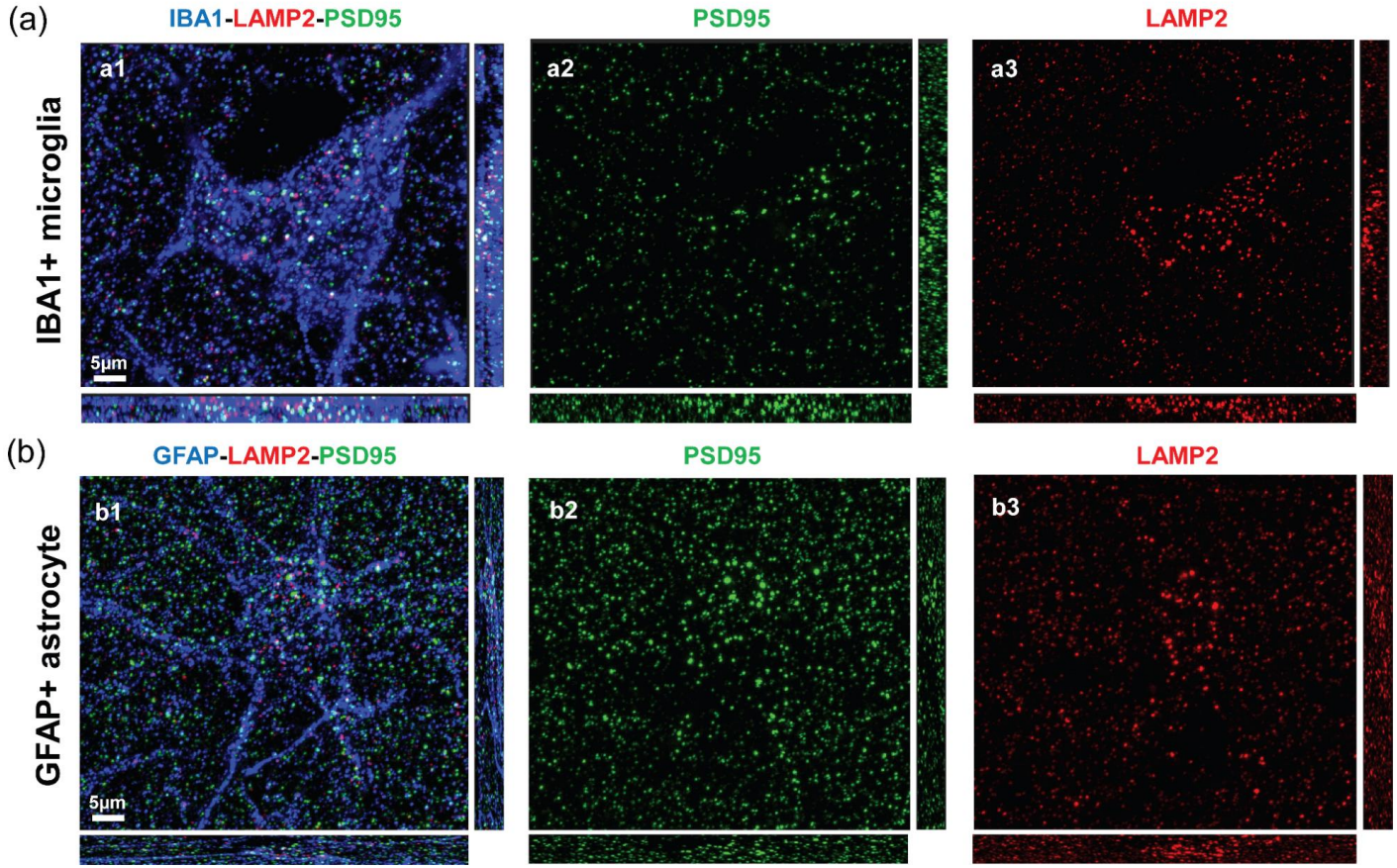

IBA1+ microglia (**a1**) and GFAP+ astrocyte (**b1**) in blue co-labelled with PSD95+ postsynapses in green (**a1/a2, b1/b2**) and LAMP2+ lysosomes in red (**a1/3, b1/3**) showing glia-internalized PSD95+ elements colocalized with LAMP2+ lysosomes inside the microglial and astrocytic cell, respectively. Scale bars 5 µm (**a**) and 10 µm (**b**).

eFigure 7. Quality of Extracted Synaptosomes and Measures of Truncated Tau

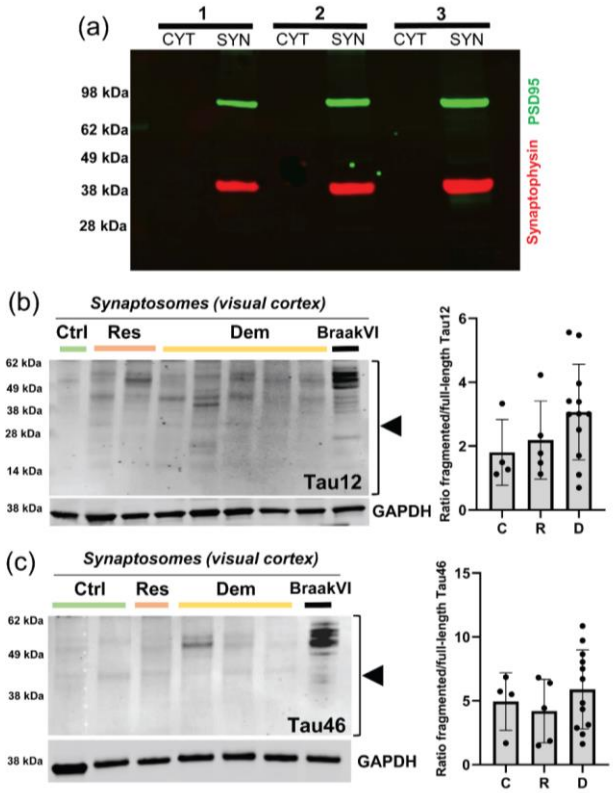

Synaptosome extractions and WB validation showing representative cytosolic (CYT) and synaptosome (SYN) fractions from three cases (1-3) using the presynaptic marker Synaptophysin (red) and the postsynaptic marker PSD95 (green) (a); WB analyses of synaptosome-enriched fractions from the visual cortex showed that tau truncation, as measured with N-terminal tau (Tau12) (b) and C-terminal tau (Tau46) (c), did not differ across demented, resilient, and control brains. Of note, WBs of synaptosome-enriched fractions with ptau217 showed no detectable signal and with AT180/ptau231 showed no difference across groups. Analyses were performed on N=21 synaptosome extractions (4 controls, 5 resilient, 12 demented), respectively. Arrowheads in black indicate the band width quantified for each of the WB analyses and respective antibodies; C/Ctrl Control (Braak 0-II); R/Res Resilient (Braak III/IV); D/Dem Demented (Braak III/IV); N:number; WB: Western Blot.

eFigure 8. Association of Oligomeric Tau With Synaptic Elements

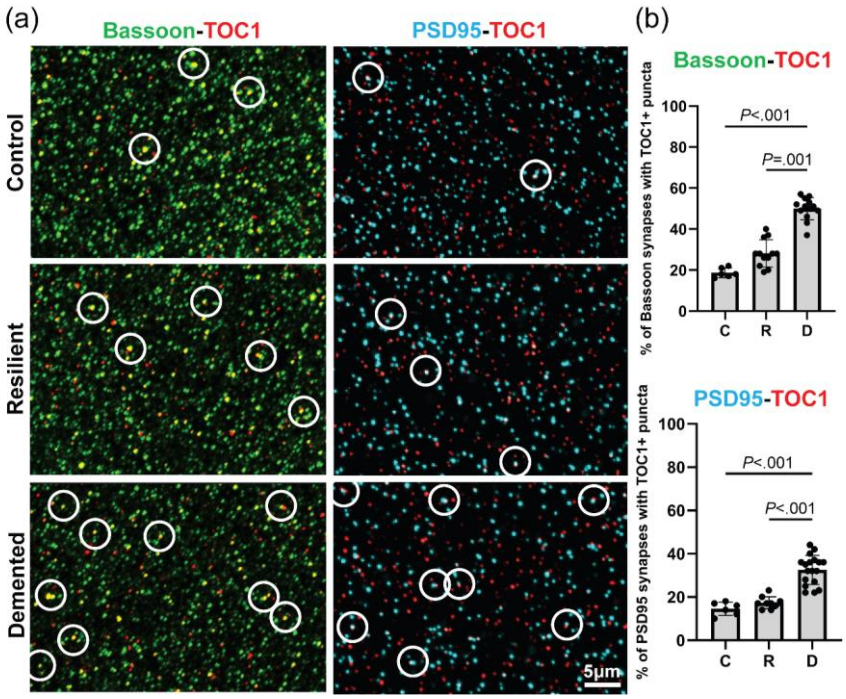

TOC1+ tau oligomers were significantly increased in Bassoon+ presynapses and PSD95+ postsynapses of demented compared to resilient and control brains (a, b). Representative images showing colocalized Bassoon+/TOC1+ presynaptic puncta (white circles) in control, resilient and demented brains (a, first column) and colocalized PSD95+/TOC1+ postsynaptic puncta (white circles) in demented, resilient, and control brains (a, second column). Analyses were performed on N=10 brains (2 controls, 4 resilient, 4 demented); C Control (Braak 0-II); R Resilient (Braak III/IV); D Demented (Braak III/IV). Scale bar 5 µm. Respective p-values are shown in the graphs.